J Sol-Gel Sci Technol (2007) 44:153–159
DOI 10.1007/s10971-007-1606-y

ORIGINAL PAPER

A high energy X-ray diffraction study of sol–gel derived $(Ta_2O_5)_x(SiO_2)_{1-x}$ glasses (x = 0.05, 0.11 and 0.25)—elucidating the role of tantalum in silica

Victoria FitzGerald · David M. Pickup · Kieran O. Drake · Mark E. Smith · Robert J. Newport

Received: 11 May 2007 / Accepted: 12 July 2007 / Published online: 16 August 2007

Abstract High energy X-ray diffraction (HEXRD) has been used to study the atomic structure of $(Ta_2O_5)_x(SiO_2)_{1-x}$ (x = 0.05, 0.11 and 0.25) xerogels; the direct interpretation of the resultant data has been augmented using reverse Monte Carlo (RMC) modelling. For the first time in this type of material, two Ta–O correlations have been identified (at ~1.8 Å and 2.0 Å). The RMC modelling approach explicitly used MAS-NMR data to define its constraints; when combined with HEXRD data, it helps to confirm the more directly determined total coordination of five for the two Ta–O correlation distances and suggests Ta···Si and Ta···Ta coordination distances of ~3.3 Å and ~3.8 Å, respectively. The O···O and Si···Si distances and coordination numbers associated with the host silica network suggest that the Ta (V) is acting as a network modifier. The way in which the Ta–O correlations are affected by composition and calcination temperature suggest some phase separation in the $(Ta_2O_5)_{0.25}(SiO_2)_{0.75}$ sample. However, in general, the results indicate good mixing of the component oxides.

Keywords High energy X-ray diffraction · Reverse Monte Carlo modelling · Tantalum · Xerogels

PACS 61.10.-i · 61.43.Fs · 81.20.Fw

V. FitzGerald (✉) · D. M. Pickup · R. J. Newport
School of Physical Sciences, University of Kent, Canterbury CT2 7NH, UK
e-mail: vf22@kent.ac.uk

K. O. Drake · M. E. Smith
Department of Physics, University of Warwick, Coventry CV4 7AL, UK

1 Introduction

$(Ta_2O_5)_x(SiO_2)_{1-x}$ mixed oxide materials have attracted interest because of their technologically relevant properties. The sol–gel route from alkoxide precursors [1] has been used to prepare such materials because it offers a low-temperature synthesis route to materials with high purity and homogeneity. $(Ta_2O_5)_x(SiO_2)_{1-x}$ mixed oxides prepared this way possess high refractive indices, rendering them suitable for optical components such as micro-lenses and optical fibres [2, 3]. The high refractive index of a given sample has been shown to depend upon the level of atomic mixing of the two oxides, a property which in turn is sensitive to the material processing. These materials also exhibit catalytic activity, which derives from the acidity of the Ta–O–Si linkages present in their structures [4]. Although the focus of this paper is entirely upon the atomic-scale structure of a specific set of $(Ta_2O_5)_x(SiO_2)_{1-x}$ sol–gel prepared mixed oxides, it is hoped that the results presented herein will be of direct interest and benefit in the broader context.

In a previous paper we reported the results of a combination of ^{29}Si and ^{17}O magic angle spinning (MAS) NMR, EXAFS and FT-IR spectroscopy to examine the local environment of tantalum and the degree of atomic mixing in these materials [5]. On the basis of the ^{29}Si MAS NMR results, which give information concerning the connectivity of the host silica network [6], it was concluded that tantalum (V) acts as a network modifier. The EXAFS measurements also identified the local tantalum environment as five-coordinated (±20%) with respect to oxygen, with an average Ta–O distance of 1.92 (±0.02) Å. The ^{17}O NMR and FT-IR spectra reveal evidence for a partial phase separation of the two component oxides in some cases. On the basis of these results, it was suggested that phase

separation occurs when $x \geq 0.18$. Here the previous study is extended and corroborated by using high energy (synchrotron) X-ray diffraction (HEXRD) to examine the atomic structure on a longer length scale (i.e. to beyond nearest neighbours). Reverse Monte Carlo (RMC) modelling has been used to help in the assignment of overlapping peaks in the experimentally derived pairwise radial distribution function (RDF). The new data more clearly and rigorously defines the role of tantalum within a glassy silicate matrix and the phase separation behaviour in this system.

2 Experimental

2.1 Sample preparation

The samples were prepared using the sol–gel route from the following precursors: tetraethyl orthosilicate, TEOS (Aldrich, 98%) and tantalum (V) ethoxide, $Ta(OEt)_5$, (Aldrich, 99.98%). HCl (Fisons) was used as a catalyst to promote the hydrolysis and condensation reactions, and ethanol (Aldrich, 99.9%) was used as a mutual solvent.

The method of Yoldas [7] was used to promote homogeneity within the mixed oxide samples. This involved pre-hydrolysis of the TEOS to maximise the number of Si–OH groups before mixing with the more reactive $Ta(OEt)_5$ precursor; the aim being to encourage Ta–O–Si bonding as opposed to Ta–O–Ta bonding which could lead to phase separation. The chosen pre-hydrolysis conditions were TEOS:EtOH:H_2O in a 1:1:1 molar ratio in the presence of HCl (pH = 1), stirring for 2 h. The appropriate quantity of $Ta(OEt)_5$ was then slowly added to the pre-hydrolysed TEOS solution whilst stirring. After allowing several minutes for the oxide precursors to mix, water was added such that the overall molar water:alkoxide ratio was 2. The resulting clear sol was then left to gel; this typically took a few days, depending on composition. It should be noted that all reagents were loaded in a dry box under a N_2 atmosphere and transferred using syringes to avoid absorption of moisture from the atmosphere.

All samples were aged for one week before being air dried for several days, finely ground, and then pumped under vacuum for 24 h to remove any excess solvent. Heat treatments were performed at a heating rate of 5 °C min^{-1} with each set temperature maintained for 2 h. Samples were prepared with nominal compositions of $(Ta_2O_5)_x(SiO_2)_{1-x}$ where $x = 0.05$, 0.11 or 0.25 and each composition batch being sub-divided and the resultant part-batches being then heated to 250 °C or to 750 °C.

Characterisation of the samples, necessary for the analysis of the diffraction data, was carried out. The sample compositions were determined using a combination of X-ray fluorescence (XRF) spectrometry and combustion analysis. The XRF measurements, performed using a Bruker S4 X-ray fluorescence spectrometer, gave the Ta:Si ratio, whilst the combustion analysis yielded the hydrogen content associated with residual –OH and/or water. The oxygen content was estimated on the basis of charge-balancing the cations present. The densities of the samples were determined by helium pycnometry using a Quantachrome Multipycnometer. The results of this characterisation are given in Table 1.

2.2 High energy X-ray diffraction experimental method and data analysis

The high energy X-ray diffraction (HEXRD) data were collected on Station 9.1 at the synchrotron radiation source (SRS), Daresbury Laboratory, UK. The finely powdered samples were enclosed inside a 0.5 mm thick circular aluminium annulus by kapton windows and mounted within a conventional θ:2θ flat-plate instrumental set-up. The wavelength was set at $\lambda = 0.4875$ Å, and calibrated using the K-edge of an Ag foil; the wavelength was low enough to provide data to a high value of momentum transfer ($Q_{max} = 4\pi sin0/\lambda \sim 23$ $Å^{-1}$, although we note that the data was in practise truncated at $Q \approx 22$ Å in all cases in order to avoid the use of statistically poorer data at the highest scattering angles). The data were corrected using a suite of programs written in-house, but based upon the methodology of Warren [8].

The initial stage of analysis of HEXRD data from an amorphous material involves normalisation, the removal of background scattering, correction for absorption and inelastic scattering, and subtraction of the self-scattering term [9]. No correction was made to account for multiple scattering since it is a negligible effect in HEXRD from thin samples having low sample attenuation. The resultant scattered intensity, $i(Q)$, can reveal structural information by Fourier transformation to obtain the pair distribution function:

$$T(r) = T^0(r) + \int_0^\infty Qi(Q)M(Q)\sin(Qr)\, d(Q) \qquad (1)$$

where $T^0(r) = 2\pi^2 r\rho_o$ (r is the atomic separation between atoms and ρ_o is the macroscopic number density) and $M(Q)$ is a window function necessitated by the finite maximum experimentally attainable value of Q (in the present case, a Hanning function was adopted [10]). Within this nomenclature we note that the total $T(r)$ may be considered as a linear combination of all pairwise partial terms, $t_{ij}(r)$, weighted by concentration of the atom types involved and the strength of their scattering of X-rays (the form factor, see below).

Table 1 Sample characterisation on the basis of XRF, CHN combustion analysis, charge balance and helium pycnometry

Sample	Heat treatment (°C)	Ta [±0.3] (atm%)	Si [±0.3] (atm%)	O [±2.0] (atm%)	H [±2.0] (atm%)	Density [±0.2] (kg m^{-3})	RMC box side (nm)
$(Ta_2O_5)_{0.05}(SiO_2)_{0.95}$	750	2.8	21.9	59.0	16.3	2540	3.00
$(Ta_2O_5)_{0.11}(SiO_2)_{0.89}$	250	3.6	13.1	50.9	31.4	2650	N/A
$(Ta_2O_5)_{0.11}(SiO_2)_{0.89}$	750	5.2	19.0	59.3	16.4	3040	2.99
$(Ta_2O_5)_{0.25}(SiO_2)_{0.75}$	750	8.9	13.3	58.6	19.2	3840	2.94

Structural information can be obtained from the diffraction data by simulating the Q-space data and converting the results to r-space by Fourier transformation to allow comparison with the experimentally determined correlation function, and iterating the process [11]. The Q-space simulation is generated using the following equation:

$$p(Q)_{ij} = \frac{N_{ij} w_{ij}}{c_j} \frac{\sin QR_{ij}}{QR_{ij}} \exp\left[\frac{-Q^2\sigma_{ij}^2}{2}\right] \quad (2)$$

where $p(Q)_{ij}$ is the pair function in reciprocal space, N_{ij}, R_{ij} and σ_{ij} are the coordination number, atomic separation and disorder parameter, respectively, of atom i with respect to j, c_j is the concentration of atom j, and w_{ij} is the associated weighting factor. The weighting factors are given by:

$$w_{ij} = \frac{2c_i c_j f(Q)_i f(Q)_j}{\overline{f(Q)}^2} \text{ if } i \neq j \quad (3)$$

or,

$$w_{ij} = \frac{c_i^2 f(Q)_i^2}{\overline{f(Q)}^2} \text{ if } i = j \quad (4)$$

where $f(Q)$ represents the Q-dependant X-ray form factor. Thus the analysis process uses real-space parameters describing the various $t_{ij}(r)$ in order to fit the Q-space data: we thereby circumvent the issue of truncation effects in this respect.

2.3 RMC method

RMC is a method for producing three-dimensional models of a structure that agree quantitatively with the available diffraction data. A starting model of a material, composed of atoms in a box at the correct density and composition, is modified by random processes in such a way as to improve the agreement between a set of experimental data and the equivalent function calculated from the model. The structure is modified in this way until it agrees with the experimental data within some satisfactory measure of the error. A full description of the RMC method can be found in a paper by the method's originator [12]. Using the diffraction data, together with a set of constraints derived from prior chemical knowledge and our existing MAS NMR data [5], a three-dimensional model has been produced for three of the sample compositions. We stress that this has been undertaken with the sole aim of informing our interpretation of the experimental data: the RMC modelling process is therefore not exhaustive, but is nevertheless useful in a heuristic sense. The RMC box for the $(Ta_2O_5)_{0.25}(SiO_2)_{0.75}$ model is made up of 2,000 atoms, with correct atomic number density and composition obtained from pycnometry measurements and X-ray fluorescence composition analysis, respectively, as per Table 1. Charge balancing was also used as an aid to building a box with the correct composition. Thus the starting configuration contained atoms of Ta, Si, O and H in direct proportion to the percentages shown in Table 1; the size chosen for the associated cubic box is determined in order to match the measured density, and is also shown in Table 1. The initial (pseudo-random) box then had several constraints imposed on it to ensure a properly configured basic silica host network. These constraints included limiting the closest approach of pairs of atoms (known as hard-sphere radii), ensuring that each Si atom had four oxygen nearest-neighbour atoms, imposing a Q-speciation distribution on the connectivity of the SiO_4 tetrahedra consistent with the results of a previous ^{29}Si NMR study on these samples [5] and ensuring that all the hydrogen is present as network terminating –OH groups.

Only when the initially random box of atoms satisfied the above constraints to a satisfactory level (>98%) was the data added as the final additional constraint. After the ratio of successful to failed moves of the atoms within the box falls to its equilibrium value, about which it will fluctuate, the model was deemed to have reached a dynamic equilibrium.

3 Results

Figures 1 and 2 show the HEXRD data from the $(Ta_2O_5)_x(SiO_2)_{1-x}$ (x = 0.05, 0.11 and 0.25) samples after Fourier transformation into r-space, together with the fit to the pair distribution function obtained using the method

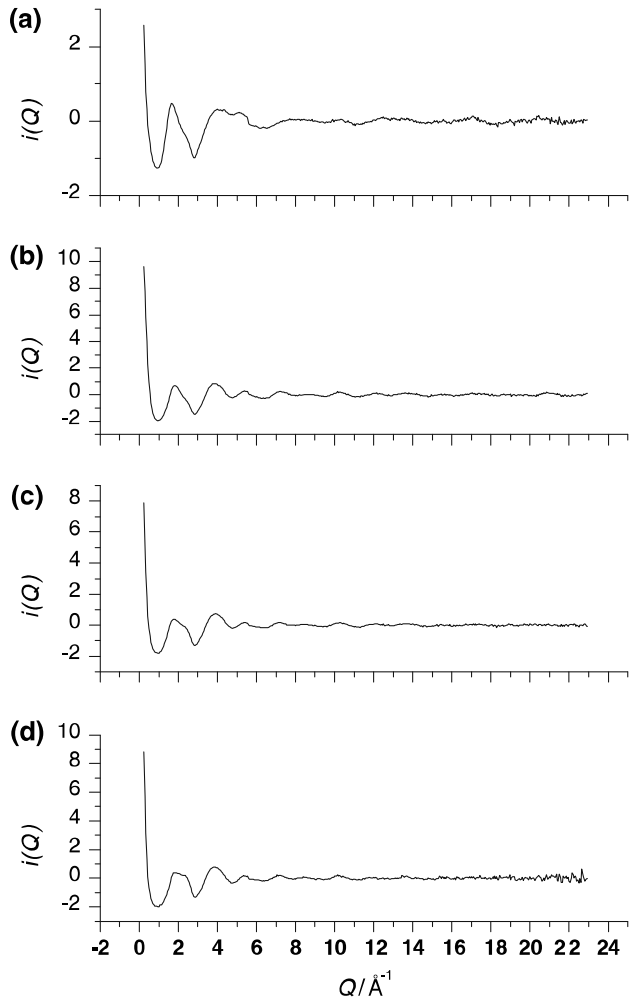

Fig. 1 High energy X-ray diffraction Q-space interference functions, $i(Q)$'s, (**a**) $(Ta_2O_5)_{0.05}(SiO_2)_{0.95}$ sample heated to 750 °C, (**b**) $(Ta_2O_5)_{0.11}(SiO_2)_{0.89}$ sample heated to 250 °C, (**c**) $(Ta_2O_5)_{0.11}(SiO_2)_{0.89}$ sample heated to 750 °C and (**d**) $(Ta_2O_5)_{0.25}(SiO_2)_{0.75}$ sample heated to 750 °C

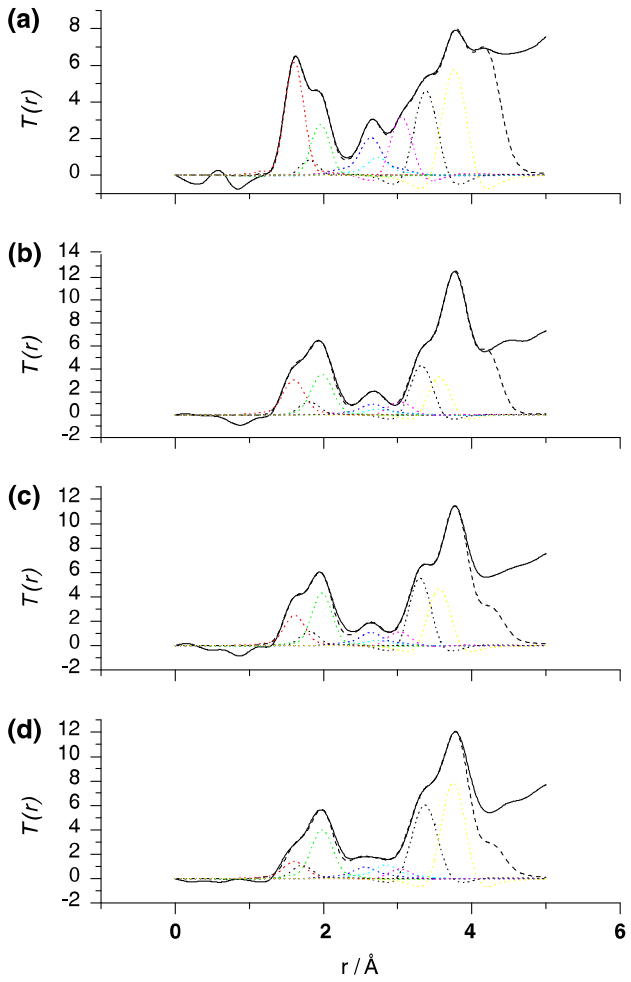

Fig. 2 High energy X-ray diffraction pair distribution functions, $T(r)$'s, (solid line) together with fit (dashed line), (**a**) $(Ta_2O_5)_{0.05}(SiO_2)_{0.95}$ sample heated to 750 °C, (**b**) $(Ta_2O_5)_{0.11}(SiO_2)_{0.89}$ sample heated to 250 °C, (**c**) $(Ta_2O_5)_{0.11}(SiO_2)_{0.89}$ sample heated to 750 °C and (**d**) $(Ta_2O_5)_{0.25}(SiO_2)_{0.75}$ sample heated to 750 °C. Partial $T(r)$ functions are also shown as dotted lines, the most important ones shown in colour as Si–O (red), Ta–O (green), O–Si–O (blue), O–Ta–O (cyan), Si···Si (magenta) and Ta···Ta (yellow). Individual partial functions may be identified by referring to Table 2

described in Sect. 2.2 above. The use of a window function in Fourier transformation is shown to have reduced truncation effects to a low level; the possible detrimental effects of the finite Q-range have been further tested, and shown not to be significant, by examining the changes at $r > 1$ Å as a result of using no window function or of truncating the data at a lower Q_{max}. We note again that we circumvent the issue of truncation effects in generating the final structural parameters gained by fitting the HEXRD data itself by adopting the methodology of Gaskell [11] and simulating in Q-space.

Three distinct features are observed in all four pair distribution functions. The broad, partially resolved split peak centred at around 1.8 Å is associated with Si–O (1.61 Å) and Ta–O (~1.95 Å) pairwise correlations, the peak at ~2.7 Å is assigned to the O···O nearest-neighbour distance and the peak at ~3.7 Å is due to a Ta···Ta distance. Also, a feature is observed at ~3.4 Å which appears as a separate peak in the $T(r)$ from the $(Ta_2O_5)_{0.11}(SiO_2)_{0.89}$ 750 °C sample and as a shoulder in the pair distribution functions of other samples; this correlation is assigned to the Ta···Si distance. The assignments of the Si–O and O···O correlations are made on the basis of previous HEXRD results from metal-doped sol–gel derived silica glass [13], and the assignment of the distances involving tantalum is consistent with the EXAFS results obtained from these materials [5]. The interpretation of this direct experimental information may now be augmented by the RMC models derived herein (the RMC fit to one data set is shown in Fig. 3). Indeed, the RMC models explicitly reveal the likelihood that the first-shell Ta–O correlation

comprises two separate Ta–O correlation distances, suggesting a distorted square pyramidal environment. Furthermore, given the problem of overlapping pairwise coordination spheres in a multi-component material of this type, the RMC method becomes useful not only in terms of peak positions and areas per se, but also with particular regard to peak assignments. Thus, all of the distances and coordination numbers shown below were initially derived on the basis of a heuristic RMC fit to the data, but were then used as the starting values for a final simulation process using the HEXRD data itself using the methodology outlined in Sect. 2.2. Table 2 shows the final parameters derived from this hybrid approach.

It is evident, on the basis of the HEXRD-derived structural parameters shown in Table 2, that significant structural changes are occurring in these materials, both as a function of composition and temperature of thermal processing. All samples show a peak at 1.61 Å with a coordination of ~4. (We note the fact that the coordination number is on average slightly higher than four as simulated; this is probably associated with residual uncertainties in sample density and composition (e.g. –OH content), which will affect the peak areas—though not peak positions—directly. Naturally, all other simulated coordination numbers are also likely therefore to be marginally higher than they ought to be.) In the $(Ta_2O_5)_{0.05}(SiO_2)_{0.95}$ and $(Ta_2O_5)_{0.11}(SiO_2)_{0.89}$ samples we obtain an O–Si–O peak as expected at 2.64 Å and a coordination of ~5. However, in the $(Ta_2O_5)_{0.25}(SiO_2)_{0.75}$ sample the distance has shortened to 2.54 Å with a coordination of ~5. All samples have a Si···Si distance of ~3.03 Å as expected and a coordination of ~4, however this coordination decreases as the concentration of Ta increases, as might be anticipated. In the $(Ta_2O_5)_{0.05}(SiO_2)_{0.95}$ sample, the Si···Ta peak is at 3.38 Å with a coordination of ~6. As the amount of Ta in the sample increases, the correlation peak distance shortens and the coordination number lowers. In all samples the Ta appears to be five-fold coordinated, with the RMC results adding the suggestion that the first coordination sphere comprises ~1 oxygen at a shorter distance and ~4 oxygen at a longer distance. In the $(Ta_2O_5)_{0.05}(SiO_2)_{0.95}$ sample the O–Ta–O peak is at 2.73 Å with a coordination of ~3, whereas in the $(Ta_2O_5)_{0.25}(SiO_2)_{0.75}$ sample the peak distance is 2.80 Å with a coordination of ~7. Lastly, the Ta···Ta peak is observed to be situated at 3.76 Å in the $(Ta_2O_5)_{0.05}(SiO_2)_{0.95}$ sample with a coordination of ~3. In the $(Ta_2O_5)_{0.11}(SiO_2)_{0.89}$ sample data one sees two Ta···Ta peaks of 3.56 Å and 3.80 Å with a total coordination of ~4. In the $(Ta_2O_5)_{0.25}(SiO_2)_{0.75}$ sample the data again shows two Ta···Ta distances of 3.50 Å and 3.80 Å with a total coordination of ~4.

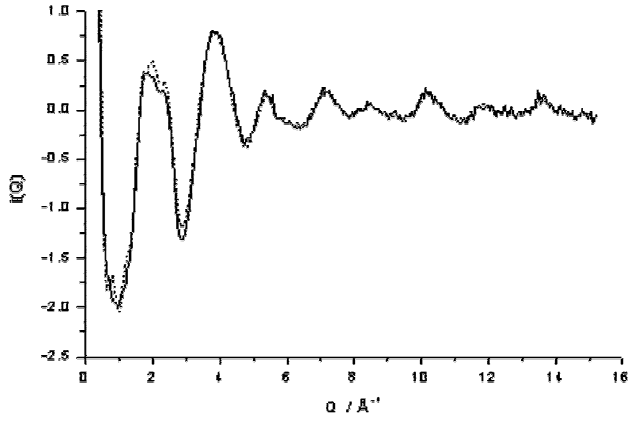

Fig. 3 RMC results for the $(Ta_2O_5)_{0.25}(SiO_2)_{0.75}$ sample heated to 750 °C: *Q*-space interference function (solid line) and RMC fit (dashed line)

4 Discussion

The results in Table 2 show that three pairwise correlations characteristic of the host silica network are present in the data presented here: the Si–O bond at 1.61 Å, the O–Si–O nearest-neighbour distance at 2.64 Å and the Si–O–Si nearest-neighbour distance at 3.03 Å. All samples exhibit a Si–O coordination number of close to four, which is as anticipated for silica-based materials [14].

The O–Si–O coordination number would tend towards six in a fully densified silica network, but in these samples calcined at 750 °C the coordination numbers are in the range of 4–5, and for the sample calcined at only 250 °C this value reduces to ~3. Taken with the composition information, this result suggests significant disruption to the network structure by the presence of hydroxyl groups (as well any effect of the tantalum ions). Such a reduction in O–Si–O coordination number from the ideal value has previously been observed in TiO_2–SiO_2 sol–gel derived glasses [13]. Furthermore, the results show a general trend of decreasing O–Si–O coordination number with increasing tantalum content. It is noted that the $(Ta_2O_5)_{0.25}(SiO_2)_{0.75}$ sample does not appear to follow this trend, possibly because the distance simulated for the O–Si–O correlation is slightly shorter, and a second peak corresponding to the O–Ta–O correlation is observed. Given that the samples calcined at the same temperature contain approximately the same concentration of hydrogen, and assuming that most of this hydrogen is in the form of hydroxyl groups, the trend of decreasing O–Si–O coordination number with tantalum concentration can be taken as evidence of Ta (V) acting as a network modifier. This conclusion is in agreement with the results of the previous ^{29}Si NMR study on the same samples, which demonstrated a reduction in connectivity of the silica network with increasing tantalum content [5].

Table 2 Structural parameters for the $(Ta_2O_5)_x(SiO_2)_{1-x}$ sol–gel samples obtained by simulating the high energy X-ray diffraction pair distribution functions. Note that the errors are ±0.02 Å in R, ±15% in N and ±0.01 Å in σ

Sample	Heat treatment (°C)	Correlation	R (Å)	N	σ (Å)	R (Å) (RMC)	N (RMC)
$(Ta_2O_5)_{0.05}(SiO_2)_{0.95}$	750	Si–O	1.61	4.5	0.04	1.61	3.39
		Ta–O	1.81	1	0.06	1.81	1
		Ta–O	1.96	4	0.08	1.95	4
		O···O	2.64	5	0.08	2.55	5.3
		O···O	2.73	2.5	0.08		
		Si···Si	3.05	4.6	0.07	3.05	3.6
		Ta···Si	3.38	6.6	0.12	3.39	3.3
		Ta···Ta	3.76	3.2	0.15	3.80	0.61
$(Ta_2O_5)_{0.11}(SiO_2)_{0.89}$	250	Si–O	1.60		4.0		0.07
		Ta–O	1.81		1.1		0.08
		Ta–O	1.98		4.1		0.10
		O···O	2.66		3.3		0.09
		O···O	2.74		1.8		0.09
		Si···Si	3.03		3.0		0.10
		Ta···Si	3.32		4.0		0.10
		Ta···Ta	3.56		1.0		0.11
		Ta···Ta	3.80		2.9		0.13
$(Ta_2O_5)_{0.11}(SiO_2)_{0.89}$	750	Si–O	1.61	4.2	0.05	1.61	3.5
		Ta–O	1.81	1.0	0.07	1.81	0.9
		Ta–O	1.98	4.3	0.08	2.00	4.0
		O–O	2.64	4.6	0.08	2.55	5.2
		O–O	2.73	2.1	0.09		
		Si···Si	3.02	3.9	0.09	3.05	3.3
		Ta···Si	3.30	4.6	0.09	3.27	2.4
		Ta···Ta	3.56	1.4	0.12	3.56	2.2
		Ta···Ta	3.80	2.8	0.12	3.80	
$(Ta_2O_5)_{0.25}(SiO_2)_{0.75}$	750	Si–O	1.61	4.0	0.05	1.63	3.72
		Ta–O	1.71	0.8	0.08	1.71	1
		Ta–O	1.98	4.1	0.09	2.00	4
		O···O	2.54	5.3	0.09	2.55	5.4
		O···O	2.80	6.8	0.09		
		Si···Si	3.03	3.8	0.08	3.05	2.6
		Ta···Si	3.26	3.5	0.12	3.25	3.9
		Ta···Ta	3.49	1.4	0.13	3.50	2.9
		Ta···Ta	3.80	3.0	0.13	3.80	

The Si–O–Si coordination number exhibits a similar trend with composition, although the errors associated with this parameter are much larger because this Si···Si first neighbour correlation is not resolved in the pair distribution functions themselves.

All the samples exhibit two Ta–O distances with a total coordination number of between 5 and 6. Previously, EXAFS measurements determined the tantalum environment in these materials to be predominantly five-fold coordinate with respect to oxygen, with a single Ta–O distance of 1.92 Å. Here, a splitting to the first-shell Ta–O environment is suggested in such materials. The $(Ta_2O_5)_{0.05}(SiO_2)_{0.95}$ and $(Ta_2O_5)_{0.11}(SiO_2)_{0.89}$ samples appear to have a longer Ta–O distance at ∼1.98 Å with a coordination of ∼4, and a shorter distance of 1.81 Å with a coordination of ∼1. By contrast, the $(Ta_2O_5)_{0.25}(SiO_2)_{0.75}$ sample, i.e. the sample having the highest Ta content, has a longer Ta–O distance at ∼1.98 Å with a coordination of ∼4, and a shorter distance of 1.71 Å with a coordination of ∼1. A distorted five-fold square pyramidal environment has been observed previously by Arakcheeva et al., studying the structures of Ta-bronzes and Ta-compounds [15]. A square pyramidal environment was also observed by Hoppe and Wehrum [16] in pentasodium tantalite; they

observed a square pyramidal environment with two Ta–O bond distances at ~2.00 Å, two at ~1.93 Å and one at 1.88 Å. Over all four samples here, the average total Ta–O first-shell coordination number measured is 5.1, which is broadly consistent with that found on the basis of less well resolved EXAFS data and supports the overall proposal that the environment of tantalum in these materials in predominantly five-fold coordinated. However, given the uncertainties in both the empirical simulation approach and in RMC modelling, one could not claim that the variations in the Ta–O coordination number between samples are themselves significant.

The RMC model plays a useful role in assignment of the peaks in the $T(r)$ functions at ~3.3 Å and ~3.8 Å to Ta···Si and Ta···Ta correlations, respectively. The RMC model also suggests a shorter Ta···Ta peak at ~3.6 Å in samples with $x \geq 0.11$, and which is possibly also present in the $x = 0.05$ sample but cannot be seen clearly due to the low number of Ta atoms in the model box.

Comparing the Ta-rich $(Ta_2O_5)_{0.25}(SiO_2)_{0.75}$ sample with the $(Ta_2O_5)_{0.05}(SiO_2)_{0.95}$ sample, one observes a clear difference, reflecting the changes observed directly in the XRD data. The Si···Ta peak is shorter in the $(Ta_2O_5)_{0.25}(SiO_2)_{0.75}$ sample, and the two Ta–O peaks, and also the Ta···Ta peaks, are clearly different in each sample, becoming more clearly resolved as the Ta content increases. The data from the $(Ta_2O_5)_{0.11}(SiO_2)_{0.89}$ samples give an indication of the effect of processing temperature. The only significant change between the results for this composition after heating to 250 °C and then 750 °C is an increase in the Si···Si, Ta···Si and Ta···Ta coordination with temperature. This is almost certainly due to the anticipated densification of the glass network via the loss of hydroxyl groups.

The results in Table 2 are consistent with partial phase segregation of the $(Ta_2O_5)_{0.25}(SiO_2)_{0.75}$ sample into component oxides. We observe in the data from this sample the evident separation of the O–Si–O and O–Ta–O distances and an increase in coordination. These changes are consistent with the presence of amorphous tantalum oxide, a-Ta_2O_5, which has been proposed to exist at this tantalum concentration on the basis of ^{17}O NMR and FT-IR results [5]. These changes are not seen in the samples of lower Ta concentration; however, the uncertainties in the results allow for there to be a minor (i.e. undetected) level of heterogeneity in all samples calcined at 750 °C. Moreover, it is noteworthy that the O···O distances and coordination numbers determined from the $(Ta_2O_5)_{0.25}(SiO_2)_{0.75}$ sample (2.54 Å and 2.80 Å, and 12 atoms, respectively) differ significantly compared to those obtained from the lower tantalum content samples (i.e. 2.64 Å and 2.73 Å, and 8 atoms): the correlation distances are seen to be shifted (separated further) and the coordination numbers increase in the way expected if the Ta–O distances change in the way described above.

5 Conclusions

The results of the first HEXRD study of $(Ta_2O_5)_x(SiO_2)_{1-x}$ sol–gel derived glass are presented. The interpretation of the experimental results is informed by a RMC modelling study incorporating experimentally determined composition and density values together with bonding constraints determined by solid state MAS-NMR. It is concluded on the basis of the above data and prior published data that, when tantalum is added to silica via the sol–gel route, it acts as a network modifier, adopting a distorted five-fold square pyramidal environment. Good mixing between the component oxides is observed at the lower Ta contents, with signs of partial phase separation observed for the $x = 0.25$ sample.

Acknowledgements The EPSRC is thanked for funding this work through Grants GR/N64151/01 and GR/N64267/01 and the CCLRC for access to the SRS facility at their Daresbury Laboratory. We are grateful to Dr A. Lennie and Dr S. Teat for their help in using the 9.1 diffractometer at the SRS. VF thanks the EPSRC and the University of Kent for her studentship.

References

1. Brinker CJ, Scherer WG (1990) Sol–gel science: the physics and chemistry of sol–gel processing. Academic, San Diego, CA
2. Satoh S, Susa K, Matsuyama I (1992) J Non-Cryst Solids 146:121
3. Satoh S, Susa K, Matsuyama I (2002) J Non-Cryst Solids 306:300
4. Guiu G, Grange P (1995) J Catal 156:132
5. Pickup DM, Mountjoy G, Holland MA, Wallidge GW, Newport RJ, Smith ME (2000) J Mater Chem 10:1887
6. MacKenzie KJD, Smith ME (2002) Multinuclear solid-state NMR of inorganic materials. Pergamon Press
7. Yoldas BE (1980) J Non-Cryst Solids 38:81
8. Warren BE (1990) X-ray diffraction. Dover Publications, New York
9. Cole JM, van Eck ERH, Mountjoy G, Anderson R, Brennan T, Bushnell-Wye G, Newport RJ, Saunders GA (2001) J Phys Condens Matter 13:4105
10. Blackman RB, Tukey JW (1959) In: The measurement of power spectra from the point of view of communications engineering. Dover, New York
11. Gaskell PH (1991) In: Zrzycky J (ed) Materials science and technology, vol 9. VCH, Weinhaim, p 175
12. McGreevy RL (2001) J Phys Condens Matter 13:887
13. Pickup DM, Mountjoy G, Roberts MA, Wallidge GW, Newport RJ, Smith ME (2000) J Phys Condens Matter 12:3521
14. Wright AC (1993) In: Simmons CJ, El-Bayoum OH (eds) Experimental techniques of glass science. The American Ceramic Society, p 218
15. Arakcheeva AV, Chapuis G, Grinevich VV, Shamrai VF (2004) Kristallografiya 49:75
16. Hoppe R, Wehrum G (1992) Zeitschrift fuer Anorganische und Allgemeine Chemie 614:38